AIMS Mathematics, 8(4): 8680–8701.
DOI: 10.3934/math.2023436
Received: 29 November 2022
Revised: 11 January 2023
Accepted: 17 January 2023
Published: 07 February 2023

http://www.aimspress.com/journal/Math

Research article

Coronavirus dynamics, infections and preventive interventions using fractional-calculus analysis

Salah Boulaaras[1],*Ziad Ur Rehman[2], Farah Aini Abdullah[3], Rashid Jan[2], Mohamed Abdalla[4] and Asif Jan[5]

[1] Department of Mathematics, College of Sciences and Arts, ArRass, Qassim University, Saudi Arabia

[2] Department of Mathematics, University of Swabi, Swabi 23561, Pakistan

[3] School of Mathematical Sciences, Universiti Sains Malaysia, 11800 USM Penang, Malaysia

[4] Mathematics Department, College of Science, King Khalid University, Abha, Saudi Arabia

[5] Department of Pathogenic Microbiology Immunology, School of Basic Medical Sciences, Xiaan Jiaotong University, Xiaan 710061, China

* **Correspondence:** Email: saleh_boulaares@yahoo.fr.

Abstract: In this research work, we construct an epidemic model to understand COVID-19 transmission vaccination and therapy considerations. The model's equilibria were examined, and the reproduction parameter was calculated via a next-generation matrix method, symbolized by $\mathcal{R}_0$. We have shown that the infection-free steady state of our system is locally asymptotically stable for $\mathcal{R}_0 < 1$. Also, the local asymptotic stability of the endemic steady state has been established for $\mathcal{R}_0 > 1$. We have used a partial rank correlation coefficient method for sensitivity analysis of the threshold parameter $\mathcal{R}_0$. The contribution of vaccination to the threshold parameter is explored through graphical results. In addition to this, the uniqueness and existence of the solution to the postulated model of COVID-19 infection is shown. We ran various simulations of the proposed COVID-19 dynamics with varied input parameters to scrutinize the complex dynamics of COVID-19 infection. We illustrated the variation in the dynamical behavior of the system with different values of the input parameters. The key factors of the system are visualized for the public health officials for the control of the infection.

Keywords: COVID-19 infection; mathematical model; vaccination; fractional dynamics; stability results; dynamical behavior
Mathematics Subject Classification: 4C05, 92D25

1. Introduction

It is significant that the World Health Organization (WHO) has identified the infection of COVID-19 as a global epidemic. This viral infection is dangerous and has symptoms that range from those of an ordinary cold to disastrous respiratory disorders. It is also reported that the coronavirus infection principally affects blood pressure. The central nervous system, skin, pregnancy, urinary system, gastrointestinal tract, endocrine system, peripheral nervous system, cardiovascular system and immunological system are all affected by this virus [1]. The acute respiratory syndrome (SARS-Cov-2) is caused by the COVID-19 virus, which targets the respiratory system. These are viruses that affect the respiratory system. In December, it was introduced for the first time in China. In January 2020, the WHO proclaimed SARS-Cov-2 to be pandemic [2]. Mathematical modeling is the ideal instrument for studying and understanding this complicated and demanding undertaking in order to cope with the epidemic. Because of the spreading characteristics of such occurrences, mathematical modeling has received a lot of interest. Many researchers have developed numerous models to investigate the temporal dynamics of communicable illness. Infectious diseases are the second-leading source of death on the planet [3, 4]. The authors in [3] considered an epidemic model with nonlinear incidence and relapse while the authors in [4] focused on the analysis and multi-model selection of COVID-19 infection.

Mathematical modeling is critical for studying disease management and dynamics, especially when the illness is in its early stages or there is no vaccine. The study of biological models of infectious illnesses has received a lot of interest in recent research articles. Stability theory and current system solutions are best described by mathematical language in optimizing epidemiological systems [5, 6]. In the case of COVID-19, numerous studies have been carried out to conceptualize different aspects of this viral infection. The virus might resurface if social separation is relaxed [7]. An effective, safe and widely used vaccine would eliminate the need for social isolation, but creating a COVID-19 vaccine is fraught with difficulties [8], and one is unlikely to be ready until spring 2021 at the earliest [9]. Until then, non-pharmaceutical measures such as social distancing, diagnostic testing, contact tracing and patient isolation will be used to successfully control COVID-19 [10]. In [11], the authors introduced the dynamics of COVID-19 and simulate the disease's phase-based transmissibility, moreover, they determine the threshold parameter and examine the system. Khan and Atangana [12] presented a mathematical model for the coronavirus infection and evaluated the disease's dynamical characteristics by detailing the interactions between bats and unknown hosts in brief detail [13, 14]. In [15], an epidemic model is presented for the investigation of the effectiveness of control policies through the use of a genetic algorithm. A novel approach has been used by the researchers for the investigation of the approximate solution of the dynamics of COVID-19 infection [16]. Here, we formulate the intricate dynamics of COVID-19 with treatment, reinfection and vaccination to study the intricate phenomena of this viral infection.

Fractional calculus is an extended version of classical calculus. Non-integer operators can be utilized to better comprehend physical phenomena and provide insight into mathematical models. The fractional-order derivatives are utilized to better understand the nonlocal behavior and memory. The highest levels of precision and measurement are likewise provided by fractional-order derivative models [17, 18]. It is reported that the dynamics of infection can be better understood by utilizing fractional derivatives [19, 20]. A number of fractional operators with non-singular and singular

kernels have been identified in recent investigations; moreover, these operators are successfully applied to different problems [21, 22]. In [23], the researchers formulated an epidemic model through the use of non-integer derivatives and showed that the results of fractional calculus are more accurate than ordinary systems. The stochastic dynamics of COVID-19 infection has been studied through the use of a fractional operator in a recent study [24]. The researchers in [25] examined the dynamics of COVID-19 by using of stochastic and deterministic model by applying a non-integer framework with optimized vaccination. They considered the real data of Saudi Arabia and inspected different vaccination scenarios with the help of numerical schemes. Due to the reported extraordinary properties of fractional operators, we have opted to represent the infection process of COVID-19 through the fractional framework.

The rest of the paper is organized follows. In Section 2, we present some concepts and definitions about fractional theory that are used in this work. We formulate a COVID-19 model in Section 3 and then represent the dynamics with the help of Caputo-Fabrizio (CF) derivatives. The basic reproduction number is calculated, symbolized by $\mathcal{R}_0$ and equilibria are investigated in the same section. We carried out numerical simulations to visualize the significance of the input factors to $\mathcal{R}_0$. In Section 4, by using fixed-point theory, the uniqueness and existence of the solution is discussed. Finally, the research is concluded in Section 5 of this article.

2. Fractional concepts

For the examination of our COVID-19 dynamics, we shall explain the principal notion and findings of the CF fractional operator. Below are the definitions of these key ideas:

Definition 2.1. *Let us take a function $g \in H^1(a,b)$; then, the CF fractional operator [26] with normality $\mathcal{W}(\tau)$ is given by*

$$D_t^{\hbar}(g(t)) = \frac{\mathcal{W}(\hbar)}{1-\hbar}\int_a^t g'(x)\exp\left[-\hbar\frac{t-x}{1-\hbar}\right]dx, \tag{2.1}$$

where $b > a$ and $\hbar \in [0,1]$. If $g \notin H^1(a,b)$, then we get

$$D_t^{\hbar}(g(t)) = \frac{\hbar\mathcal{W}(\hbar)}{1-\hbar}\int_a^t (g(t)-g(x))\exp\left[-\hbar\frac{t-x}{1-\hbar}\right]dx. \tag{2.2}$$

Remark 2.1. *If $\sigma = \frac{1-\hbar}{\hbar} \in [0,\infty)$ and $\hbar = \frac{1}{1+\sigma} \in [0,1]$, then from (2.2), one can get*

$$D_t^{\hbar}(g(t)) = \frac{M(\sigma)}{\sigma}\int_a^t g'(x)e^{[-\frac{t-x}{\sigma}]}dx; \tag{2.3}$$

furthermore, the below is obtained:

$$\lim_{\sigma\longrightarrow 0}\frac{1}{\sigma}\exp\Big[-\frac{t-x}{\sigma}\Big] = \delta(x-t), \tag{2.4}$$

where $M(0) = M(\infty) = 1$.

Definition 2.2. *[27] The integral of the above fractional operator is defined as follows:*

$$I_t^{\hbar}(g(t)) = \frac{2(1-\hbar)}{(2-\hbar)\mathcal{W}(\hbar)}g(t) + \frac{2\hbar}{(2-\hbar)\mathcal{W}(\hbar)}\int_0^t g(u)du, \quad t \geq 0, \tag{2.5}$$

where $0 < \hbar < 1$ *and indicates integral order:*

Remark 2.2. *The above Eq (2.2) yields the following:*

$$\frac{2(1-\hbar)}{(2-\hbar)\mathcal{W}(\hbar)} + \frac{2\hbar}{(2-\hbar)\mathcal{W}(\hbar)} = 1, \tag{2.6}$$

where $\mathcal{W}(\hbar) = \frac{2}{2-\hbar}$. *From [27], we have*

$$D_t^{\hbar}(g(t)) = \frac{1}{1-\hbar}\int_0^t g'(x)\exp\Big[\hbar\frac{t-x}{1-\hbar}\Big]dx. \tag{2.7}$$

3. Formulation of COVID-19 dynamics

We propose a mathematical model for the transmission of COVID-19 with treatment and immunization in this portion of the study, where $\mathcal{N}(t)$ is the whole population and the population has been divided into five classes: $\mathcal{S}(t)$ indicates the susceptible individuals, $\mathcal{V}(t)$ indicates the vaccinated individuals, $\mathcal{I}(t)$ indicates the infected individuals, $\mathcal{T}(t)$ indicates the treated individuals and $\mathcal{R}(t)$ denotes the recovered individuals at time t. Susceptible individuals are those who have not been infected with COVID-19, whereas infected individuals are those who have been diagnosed with COVID-19 and have transmitted the virus to the susceptible ones. People who have been treated for the illness are known to have been treated; these assumptions leads us to the following:

$$\begin{cases} \frac{d\mathcal{S}}{dt} &= \xi + \beta_1 R + \beta_2\mathcal{V} - \omega\mathcal{I}\mathcal{S} - \gamma\mathcal{S} - \mu\mathcal{S}, \\ \frac{d\mathcal{V}}{dt} &= \gamma\mathcal{S} - \beta_2\mathcal{V} - \mu\mathcal{V}, \\ \frac{d\mathcal{I}}{dt} &= \omega\mathcal{S}\mathcal{I} - \rho\mathcal{I} - \alpha\mathcal{I} - \mu\mathcal{I}, \\ \frac{d\mathcal{T}}{dt} &= \rho\mathcal{I} - \theta\mathcal{T} - \psi\mathcal{T} - \mu\mathcal{T}, \\ \frac{d\mathcal{R}}{dt} &= \psi\mathcal{T} - \beta_1\mathcal{R} - \mu\mathcal{R}, \end{cases} \tag{3.1}$$

with

$$\mathcal{N}(t) = \mathcal{S}(t) + \mathcal{V}(t) + \mathcal{I}(t) + \mathcal{T}(t) + \mathcal{R}(t),$$

and

$$\mathcal{S}(0) \geq 0, \mathcal{V}(0) \geq 0, \mathcal{I}(0) \geq 0, \mathcal{T}(0) \geq 0, \mathcal{R}(0) \geq 0.$$

The initial values of the state variables and the values of parameters are listed in the following Table 1 for numerical purposes. The flow chart of the transmission phenomena of our model is illustrated in Figure 1.

Table 1. Parameter and state variable descriptions and values per day.

Parameter	Description	Value of parameter
$\mathcal{S}$	Susceptible individuals	Assumed
$\mathcal{T}$	Treated individuals	Assumed
ξ	Recruitment rate of individuals	3.04500
ω	Transmission rate from $\mathcal{S}$ to $\mathcal{I}$	0.00143
ρ	Treatment rate of individuals	0.0034
μ	Natural death rate of individuals	0.016
γ	Rate of vaccination of individuals	0.010
α	Death resulting from COVID-19	0.0173
$\mathcal{I}$	Infected individuals	Assumed
ψ	Treated rate for recovering from COVID-19	0.003
β_1	Immunity loss rate for recovered individuals	0.005
β_2	Immunity loss rate for vaccination	0.052
$\mathcal{V}$	Vaccinated individuals	Assumed
θ	Death rate due to COVID-19	0.003
$\mathcal{R}$	Recovered individuals	Assumed

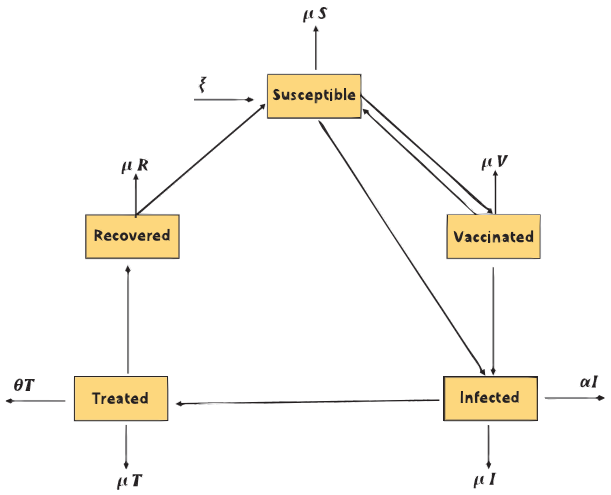

Figure 1. Illustration of the flow of the transmission of COVID-19 for our model.

Mathematical biology is one of the many uses of fractional theory in technology and science. Fractional frameworks have been shown to be more precious rather than traditional derivatives for diseases. It is reported that the recently developed CF derivative describes the nonlocal behavior of biological processes more accurately. Therefore, we represent our model of COVID-19 infection by

using a CF fractional operator as follows

$$\begin{cases} {}_0^{CF}D_t^{\hbar}\mathcal{S} &= \xi + \beta_1 R + \beta_2 \mathcal{V} - \omega \mathcal{I}\mathcal{S} - \gamma \mathcal{S} - \mu \mathcal{S}, \\ {}_0^{CF}D_t^{\hbar}\mathcal{V} &= \gamma \mathcal{S} - \beta_2 \mathcal{V} - \mu \mathcal{V}, \\ {}_0^{CF}D_t^{\hbar}\mathcal{I} &= \omega \mathcal{S}\mathcal{I} - \rho \mathcal{I} - \alpha \mathcal{I} - \mu \mathcal{I}, \\ {}_0^{CF}D_t^{\hbar}\mathcal{T} &= \rho \mathcal{I} - \theta \mathcal{T} - \psi \mathcal{T} - \mu \mathcal{T}, \\ {}_0^{CF}D_t^{\hbar}\mathcal{R} &= \psi \mathcal{T} - \beta_1 \mathcal{R} - \mu \mathcal{R}, \end{cases} \tag{3.2}$$

where $\hbar$ is the CF fractional operator's order. Next, we focus on the positive invariant region for our fractional model of Covid1-19 infection which can be easily proven by applying analytic skills [28].

Theorem 3.1. *Let us take* $\Xi = \{(\mathcal{S}, \mathcal{V}, \mathcal{I}, \mathcal{T}, \mathcal{R}) \in R_+^5 : 0 \leq \mathcal{S} + \mathcal{V} + \mathcal{I} + \mathcal{T} + \mathcal{R} \leq \mathcal{M}\}$ *where* $\mathcal{M}$ *is a positive constant; then, the set* Ξ *is positive-invariant for the above-mentioned system (9) of COVID-19.*

Investigation of the model

Now we will focus on the analysis of the suggested COVID-19 model (9) including equilibria, stability, reproduction parameter and sensitivity analysis. We indicate the disease-free equilibria by $\mathcal{E}_0$ and it is given by the following values

$$\mathcal{E}_0 = (\mathcal{S}^0, \mathcal{V}^0, \mathcal{I}^0, \mathcal{T}^0, \mathcal{R}^0) = \left(\frac{\xi(\mu + \beta_2)}{\mu(\mu + \beta_2 + \gamma)}, \frac{\gamma\xi}{\mu(\mu + \beta_2 + \gamma)}, 0, 0, 0 \right).$$

The reproduction parameter of the system can be determined by the methods mentioned in [29, 30] as follows

$$\mathcal{F} = \begin{bmatrix} \omega \frac{\xi(\mu+\beta_2)}{\mu(\mu+\beta_2+\gamma)} \end{bmatrix},$$
$$\mathcal{V} = \begin{bmatrix} \rho + \alpha + \mu \end{bmatrix},$$

which implies that

$$\mathcal{F}\mathcal{V}^{-1} = \begin{bmatrix} \frac{\omega\xi(\mu+\beta_2)}{\mu(\mu+\beta_2+\gamma)} \end{bmatrix} \begin{bmatrix} \frac{1}{\rho+\alpha+\mu} \end{bmatrix}$$
$$= \begin{bmatrix} \frac{\omega\xi(\mu+\beta_2)}{\mu(\mu+\beta_2+\gamma)(\rho+\alpha+\mu)} \end{bmatrix}.$$

Thus, the required reproduction number is given by

$$\mathcal{R}_0 = \frac{\omega\xi(\mu + \beta_2)}{\mu(\mu + \beta_2 + \gamma)(\rho + \alpha + \mu)}.$$

Theorem 3.2. *If* $\mathcal{R}_0 < 1$*, then the DFE* $\mathcal{E}_0(\mathcal{S}^0, \mathcal{V}^0, \mathcal{I}^0, \mathcal{T}^0, \mathcal{R}^0)$ *of the system (9) is stable in the local domain and unstable in other cases.*

Proof 3.2. In this case, we take the Jacobian matrix of our recommended system of COVID-19 as

$$J = \begin{bmatrix} -(\gamma + \mu) & \beta_2 & -\omega\mathcal{S}^0 & 0 & \beta_1 \\ \gamma & -(\beta_2 + \mu) & 0 & 0 & 0 \\ \omega\mathcal{I}^0 & 0 & \omega\mathcal{S}^0 - (\rho + \alpha + \mu) & 0 & 0 \\ 0 & 0 & \rho & -(\theta + \psi + \mu) & 0 \\ 0 & 0 & 0 & \psi & -(\beta_1 + \mu) \end{bmatrix}; \tag{3.3}$$

simplifying the above Eq (3.3) at the disease-free equilibrium $\mathcal{E}_0(\mathcal{S}^0, \mathcal{V}^0, \mathcal{I}^0, \mathcal{T}^0, \mathcal{R}^0)$, we obtain

$$J = \begin{bmatrix} -(\gamma+\mu) & \beta_2 & -\frac{\omega\xi(\mu+\beta_2)}{\mu(\mu+\beta_2+\gamma)} & 0 & \beta_1 \\ \gamma & -(\beta_2+\mu) & 0 & 0 & 0 \\ 0 & 0 & \frac{\omega\xi(\mu+\beta_2)}{\mu(\mu+\beta_2+\gamma)} - (\rho+\alpha+\mu) & 0 & 0 \\ 0 & 0 & \rho & -(\theta+\psi+\mu) & 0 \\ 0 & 0 & 0 & \psi & -(\beta_1+\mu) \end{bmatrix}. \tag{3.4}$$

Now, we find the roots of (3.4) as follows:

$$J = \begin{bmatrix} -(\gamma+\mu)-\lambda & \beta_2 & -\frac{\omega\xi(\mu+\beta_2)}{\mu(\mu+\beta_2+\gamma)} & 0 & \beta_1 \\ \gamma & -(\beta_2+\mu)-\lambda & 0 & 0 & 0 \\ 0 & 0 & \frac{\omega\xi(\mu+\beta_2)}{\mu(\mu+\beta_2+\gamma)} - (\rho+\alpha+\mu)-\lambda & 0 & 0 \\ 0 & 0 & \rho & -(\theta+\psi+\mu)-\lambda & 0 \\ 0 & 0 & 0 & \psi & -(\beta_1+\mu)-\lambda \end{bmatrix}. \tag{3.5}$$

Solving (3.5), we get

$$[-(\gamma+\mu)-\lambda]\,[-(\beta_2+\mu)-\lambda]\left[\frac{\omega\xi(\mu+\beta_2)}{\mu(\mu+\beta_2+\gamma)} - (\rho+\alpha+\mu)-\lambda\right][-(\theta+\psi+\mu)-\lambda]\,[-(\beta_1+\mu)-\lambda] = 0.$$

Here, the eigenvalues $-(\gamma+\mu)$, $-(\beta_2+\mu)$, $-(\beta_1+\mu)$ and $-(\theta+\psi+\mu)$ are negative. To fulfill the condition of stability, we take

$$\frac{\omega\xi(\mu+\beta_2)}{\mu(\mu+\beta_2+\gamma)} - (\rho+\alpha+\mu)-\lambda = 0,$$

which implies that

$$\lambda = \frac{\omega\xi(\mu+\beta_2)}{\mu(\mu+\beta_2+\gamma)} - (\rho+\alpha+\mu);$$

from the above, we have

$$\lambda = (\rho+\alpha+\mu)(\mathcal{R}_0 - 1),$$

which implies that the last eigenvalue λ is negative for $\mathcal{R}_0 < 1$. As a result of this, the DFE $\mathcal{E}_0(\mathcal{S}^0, \mathcal{V}^0, \mathcal{I}^0, \mathcal{T}^0, \mathcal{R}^0)$ of the system (9) is stable in the local domain if $\mathcal{R}_0 < 1$.

Let the endemic state be denoted by $\mathcal{E}_1 = (\mathcal{S}^*, \mathcal{V}^*, \mathcal{I}^*, \mathcal{T}^*, \mathcal{R}^*)$. $\mathcal{E}_1$ is obtained by setting all equations of model (9) equal to zero and solving the model; we have the following:

$$\mathcal{S}^* = \frac{\xi(\mu+\psi+\theta)(\mu+\gamma)}{\omega(\mu+\psi+\theta)},$$

$$\mathcal{V}^* = \frac{\gamma(\xi(\mu+\psi+\theta)+\beta_1\psi\rho)(\mu+\gamma)}{\omega(\mu+\psi+\theta)(\mu+\beta_2)},$$

$$\mathcal{I}^* = \frac{\mu+\psi+\theta}{(\xi(\mu+\psi+\theta)+\beta_1\psi\rho)(\mu+\gamma) - (\mu+\psi+\theta)(\mu+\rho+\alpha)},$$

$$\mathcal{T}^* = \frac{\rho}{(\xi(\mu+\psi+\theta)+\beta_1\psi\rho)(\mu+\gamma) - (\mu+\psi+\theta)(\mu+\rho+\alpha)},$$

and

$$\mathcal{R}^* = \frac{\psi\rho}{(\mu+\beta_1)(\xi(\mu+\psi+\theta)+\beta_1\psi\rho)(\mu+\gamma) - (\mu+\psi+\theta)(\mu+\rho+\alpha)}.$$

Theorem 3.3. *In the case of $\mathcal{R}_0 > 1$, the endemic steady-state $\mathcal{E}_1$ of (9) is stable in the local domain at $\mathcal{E}_1 = (\mathcal{S}^*, \mathcal{V}^*, \mathcal{I}^*, \mathcal{T}^*, \mathcal{R}^*)$.*

Proof 3.3. In this case, we use the Jacobian matrix at endemic steady state as

$$\mathcal{J}_{\mathcal{E}_1} = \begin{bmatrix} -(\omega\mathcal{I}^* + \gamma + \mu) & \beta_2 & -\omega\mathcal{S}^* & 0 & \beta_1 \\ \gamma & -(\beta_2 + \mu) & 0 & 0 & 0 \\ \omega\mathcal{I}^* & 0 & \omega\mathcal{S}^* - (\rho + \alpha + \mu) & 0 & 0 \\ 0 & 0 & \rho & -(\theta + \psi + \mu) & 0 \\ 0 & 0 & 0 & \psi & -(\beta_1 + \mu) \end{bmatrix}. \tag{3.6}$$

The fifth-order polynomial equation for $\mathcal{J}_{\mathcal{E}_1}$ is given as

$$\mathcal{P} = \lambda^5 + \mathcal{Z}_1\lambda^4 + \mathcal{Z}_2\lambda^3 + \mathcal{Z}_3\lambda^2 + \mathcal{Z}_4\lambda + \mathcal{Z}_5.$$

Here, we get

$$\mathcal{Z}_1 = \mathcal{W}_4 + \mathcal{W}_3 + \mathcal{W}_5 + (\mathcal{W}_5 + \mathcal{W}_4)\mathcal{W}_3 + \mathcal{W}_5\mathcal{W}_4 + \gamma\beta_2,$$

$$\mathcal{Z}_2 = (\mathcal{W}_4 + \mathcal{W}_3 + \mathcal{W}_5)(1 + \mathcal{W}_2 + \mathcal{W}_1) + \mathcal{W}_1\mathcal{W}_2,$$

$$\mathcal{Z}_3 = \mathcal{W}_4\mathcal{W}_3\mathcal{W}_5 + \mathcal{W}_3\gamma\beta_2 + (\mathcal{W}_2 + \mathcal{W}_1)((\mathcal{W}_5 + \mathcal{W}_4)\mathcal{W}_3 + \mathcal{W}_4\mathcal{W}_5 + \gamma\beta_2) + \mathcal{W}_2\mathcal{W}_1(\mathcal{W}_4 + \mathcal{W}_3 + \mathcal{W}_5),$$

$$\mathcal{Z}_4 = (\mathcal{W}_2 + \mathcal{W}_1)(\mathcal{W}_4\mathcal{W}_3\mathcal{W}_5 + \mathcal{W}_3\gamma\beta_2) + \mathcal{W}_2\mathcal{W}_1((\mathcal{W}_5 + \mathcal{W}_4)\mathcal{W}_3 + \mathcal{W}_4\mathcal{W}_5 + \gamma\beta_2)$$

and

$$\mathcal{Z}_5 = (\mathcal{W}_2\mathcal{W}_1(\mathcal{W}_4\mathcal{W}_3\mathcal{W}_5 + \mathcal{W}_3\gamma\beta_2) - \beta_1\psi\rho\mathcal{W}_5,$$

with the following assumptions:

$$\mathcal{W}_1 = \mu + \beta_1,$$

$$\mathcal{W}_2 = \mu + \psi + \theta,$$

$$\mathcal{W}_3 = \omega\mathcal{S}^{'} - (\mu + \rho + \alpha),$$

$$\mathcal{W}_4 = \omega\mathcal{I}^{'} + \mu + \gamma,$$

$$\mathcal{W}_5 = \mu + \beta_2.$$

Using the Routh-Hurwitz method we get the criteria for stability:

$$\mathcal{W}_i > 0 \; for \; i = 1, 2, 3, 4, 5,$$

$$\mathcal{W}_2\mathcal{W}_1\mathcal{W}_3 > \mathcal{W}_3^2 + \mathcal{W}_1^2\mathcal{W}_4,$$

$$\mathcal{W}_1\mathcal{W}_4 - (\mathcal{W}_1\mathcal{W}_2\mathcal{W}_3 - \mathcal{W}_3^2 - \mathcal{W}_1^2\mathcal{W}_4)\mathcal{W}_5 > \mathcal{W}_5(\mathcal{W}_1\mathcal{W}_2 - \mathcal{W}_3)^2 + \mathcal{W}_1\mathcal{W}_5^2.$$

As a result, the required proof is completed.

Next, we show the impact of the input factors on the reproduction number of the system $\mathcal{R}_0$ by employing a partial ranked correlation coefficient method (PRCC). The outcomes of the PRCC significance test is illustrated in Figure 2 with PRCC values of 0.7609, −0.8697, 0.3049, −0.3549, −0.3940, −0.3499 and 0.8422 for the parameters $\omega, \mu, \beta_2, \gamma, \rho, \alpha$ and ξ, respectively. This implies that the parameters μ, ξ, ω and ρ are the most sensitive parameters of $\mathcal{R}_0$ followed by the other parameters. We performed different simulations to check the results of $\mathcal{R}_0$. The outcomes of the reproduction

number are checked against variation of the transmission rate, treatment rate, vaccination rate and immunity loss rate, as can be seen in Figure 3.

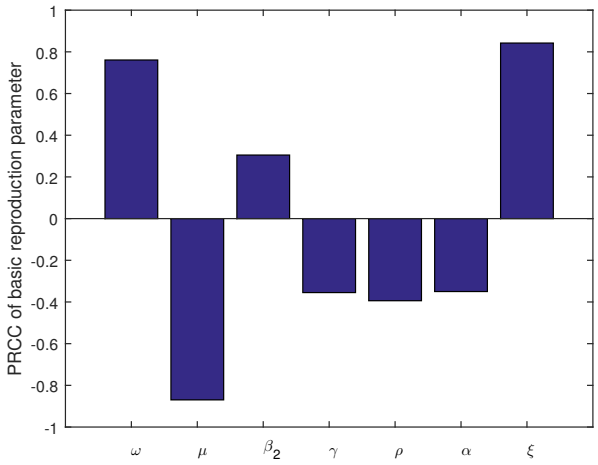

Figure 2. Illustration of the significance test results for the threshold parameter $\mathcal{R}_0$.

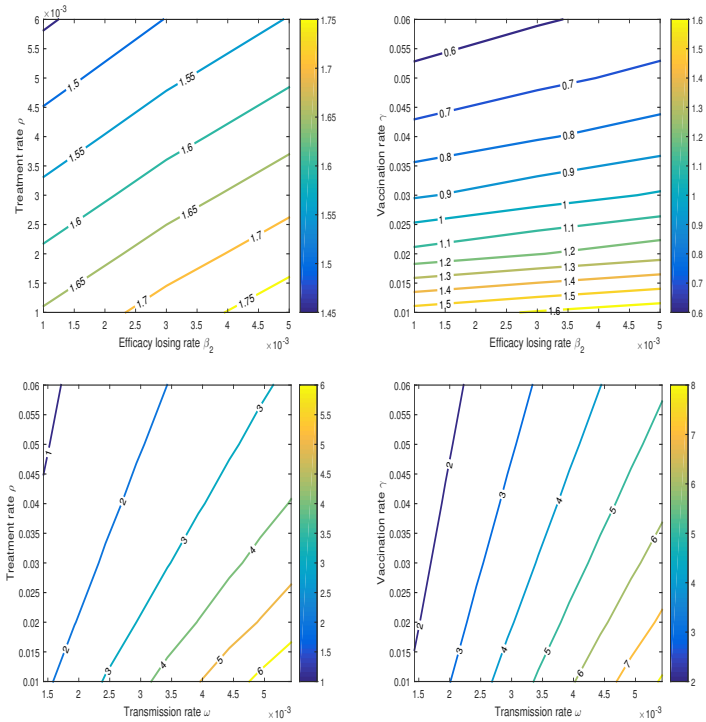

Figure 3. Graphical view analysis of the basic reproduction/threshold value in the presence of the fluctuation of various input values.

4. Solution investigation

The examination of the solutions of our COVID-19 model is the subject of this study. The presence of a solution will be investigated by using fixed-point theory (9). We will proceed as follows:

$$\begin{cases} \mathcal{S}(t)-\mathcal{S}(0) &= {}^{CF}_{0}I^{\hbar}_{t}\Big\{\xi+\beta_1\mathcal{R}+\beta_2\mathcal{V}-\omega\mathcal{I}\mathcal{S}-\gamma\mathcal{S}-\mu\mathcal{S}\Big\},\\ \mathcal{V}(t)-\mathcal{V}(0) &= {}^{CF}_{0}I^{\hbar}_{t}\Big\{\gamma\mathcal{S}-\beta_2\mathcal{V}-\mu\mathcal{V}\Big\},\\ \mathcal{I}(t)-\mathcal{I}(0) &= {}^{CF}_{0}I^{\hbar}_{t}\Big\{\omega\mathcal{S}\mathcal{I}-\rho\mathcal{I}-\alpha\mathcal{I}-\mu\mathcal{T}\Big\},\\ \mathcal{T}(t)-\mathcal{T}(0) &= {}^{CF}_{0}I^{\hbar}_{t}\Big\{\rho\mathcal{I}-\theta\mathcal{T}-\psi\mathcal{T}-\mu\mathcal{T}\Big\},\\ \mathcal{R}(t)-\mathcal{R}(0) &= {}^{CF}_{0}I^{\hbar}_{t}\Big\{\psi\mathcal{T}-\beta_1\mathcal{R}-\mu\mathcal{R}\Big\}. \end{cases} \tag{4.1}$$

Using the result of [29], we have the below

$$\begin{aligned} \mathcal{S}(t)-\mathcal{S}(0) &= \frac{2\hbar}{(2-\hbar)W(\hbar)}\int_0^t\Big\{\xi+\beta_1\mathcal{R}+\beta_2\mathcal{V}-\omega\mathcal{I}\mathcal{S}-\gamma\mathcal{S}-\mu\mathcal{S}\Big\}dy\\ &+ \frac{2(1-\hbar)}{(2-\hbar)W(\hbar)}\Big\{\xi+\beta_1\mathcal{R}+\beta_2\mathcal{V}-\omega\mathcal{I}\mathcal{S}-\gamma\mathcal{S}-\mu\mathcal{S}\Big\},\\ \mathcal{V}(t)-\mathcal{V}(0) &= \frac{2(1-\hbar)}{(2-\hbar)W(\hbar)}\Big\{\gamma\mathcal{S}-\beta_2\mathcal{V}-\mu\mathcal{V}\Big\}\\ &+\frac{2\hbar}{(2-\hbar)W(\hbar)}\int_0^t\Big\{\gamma\mathcal{S}-\beta_2\mathcal{V}-\mu\mathcal{V}\Big\}dy\\ \mathcal{I}(t)-\mathcal{I}(0) &= \frac{2(1-\hbar)}{(2-\hbar)W(\hbar)}\Big\{\omega\mathcal{S}\mathcal{I}-\rho\mathcal{I}-\alpha\mathcal{I}-\mu\mathcal{T}\Big\}\\ &+\frac{2\hbar}{(2-\hbar)W(\hbar)}\int_0^t\Big\{\omega\mathcal{S}\mathcal{I}-\rho\mathcal{I}-\alpha\mathcal{I}-\mu\mathcal{T}\Big\}dy,\\ \mathcal{T}(t)-\mathcal{T}(0) &= \frac{2(1-\hbar)}{(2-\hbar)W(\hbar)}\Big\{\rho\mathcal{I}-\theta\mathcal{T}-\psi\mathcal{T}-\mu\mathcal{T}\Big\}\\ &+\frac{2\hbar}{(2-\hbar)W(\hbar)}\int_0^t\Big\{\rho\mathcal{I}-\theta\mathcal{T}-\psi\mathcal{T}-\mu\mathcal{T}\Big\}dy,\\ \mathcal{R}(t)-\mathcal{R}(0) &= \frac{2(1-\hbar)}{(2-\hbar)W(\hbar)}\Big\{\psi\mathcal{T}-\beta_1\mathcal{R}-\mu\mathcal{R}\Big\}\\ &+\frac{2\hbar}{(2-\hbar)W(\hbar)}\int_0^t\Big\{\psi\mathcal{T}-\beta_1\mathcal{R}-\mu\mathcal{R}\Big\}dy. \end{aligned} \tag{4.2}$$

Therefore,

$$\begin{cases} P_1(t,\mathcal{S}) &= \xi+\beta_1\mathcal{R}+\beta_2\mathcal{V}-\omega\mathcal{I}\mathcal{S}-\gamma\mathcal{S}-\mu\mathcal{S},\\ P_2(t,\mathcal{V}) &= \gamma\mathcal{S}-\beta_2\mathcal{V}-\mu\mathcal{V},\\ P_3(t,\mathcal{I}) &= \omega\mathcal{S}\mathcal{I}-\rho\mathcal{I}-\alpha\mathcal{I}-\mu\mathcal{T},\\ P_4(t,\mathcal{T}) &= \rho\mathcal{I}-\theta\mathcal{T}-\psi\mathcal{T}-\mu\mathcal{T},\\ P_5(t,\mathcal{R}) &= \psi\mathcal{T}-\beta_1\mathcal{R}-\mu\mathcal{R}. \end{cases} \tag{4.3}$$

Theorem 4.1. *The kernels P_1, P_2, P_3, P_4 and P_5 satisfy the contraction and Lipschitz condition if the following is satisfied:*

$$0 \leq (\omega M + \gamma + \mu) < 1.$$

Proof. For the required result, we take $\mathcal{S}$ and $\mathcal{S}_1$ and proceed from P_1 as follows

$$P_1(t,\mathcal{S}) - P_1(t,\mathcal{S}_1) = -(\omega\mathcal{I}(\mathcal{S}(t) - \mathcal{S}(t)_1) + \gamma(\mathcal{S}(t) - \mathcal{S}(t)_1) + \mu(\mathcal{S}(t) - \mathcal{S}(t)_1)). \tag{4.4}$$

On solving (4.4), we get that

$$\begin{aligned} \|P_1(t,\mathcal{S}) - P_1(t,\mathcal{S}_1)\| &\leq \|\omega\mathcal{I}\{\mathcal{S}(t) - \mathcal{S}(t)_1\}\| + \|\gamma\{\mathcal{S}(t) - \mathcal{S}(t)_1\}\| \\ &\quad + \|\mu\{\mathcal{S}(t) - \mathcal{S}(t)_1\}\| \\ &\leq \|\omega M\|\|\{\mathcal{S}(t) - \mathcal{S}(t)_1\}\| + \gamma\|\{\mathcal{S}(t) - \mathcal{S}(t)_1\}\| \\ &\quad + \mu\|\{\mathcal{S}(t) - \mathcal{S}(t)_1\}\| \\ &\leq \omega M\|\{\mathcal{S}(t) - \mathcal{S}(t)_1\}\| + \gamma\|\{\mathcal{S}(t) - \mathcal{S}(t)_1\}\| \\ &\quad + \mu\|\{\mathcal{S}(t) - \mathcal{S}(t)_1\}\| \\ &\leq (\omega M + \gamma + \mu)\|\{\mathcal{S}(t) - \mathcal{S}(t)_1\}\|. \end{aligned} \tag{4.5}$$

Let $Q_1 = (\omega M + \gamma + \mu)$, where $\|\mathcal{I}\| \leq M$ due to boundedness; we obtain

$$\|P_1(t,\mathcal{S}) - P_1(t,\mathcal{S}_1)\| \leq Q_1\|\mathcal{S}(t) - \mathcal{S}(t)_1\|. \tag{4.6}$$

As a consequence of this, we demonstrate the Lipschitz condition for P_1, as well as the contraction resulting from the condition $0 \leq (\omega M + \gamma + \mu) < 1$. We may also determine the Lipschitz conditions in the same way.

$$\begin{aligned} \|P_2(t,\mathcal{V}) - P_2(t,\mathcal{V}_1)\| &\leq Q_2\|\mathcal{V}(t) - \mathcal{V}(t)_1\|, \\ \|P_3(t,\mathcal{I}) - P_3(t,\mathcal{I}_1)\| &\leq Q_3\|\mathcal{I}(t) - \mathcal{I}(t)_1\|, \\ \|P_4(t,\mathcal{T}) - P_4(t,\mathcal{T}_1)\| &\leq Q_4\|\mathcal{T}(t) - \mathcal{T}(t)_1\|, \\ \|P_5(t,\mathcal{R}) - P_5(t,\mathcal{R}_1)\| &\leq Q_5\|\mathcal{R}(t) - \mathcal{R}(t)_1\|. \end{aligned} \tag{4.7}$$

Further, solving (4.2) shows that

$$\begin{cases} \mathcal{S}(t) = \mathcal{S}(0) + \frac{2(1-\hbar)}{(2-\hbar)W(\hbar)}P_1(t,\mathcal{S}) + \frac{2\hbar}{(2-\hbar)W(\hbar)}\int_0^t (P_1(y,\mathcal{S}))dy, \\ \mathcal{V}(t) = \mathcal{V}(0) + \frac{2(1-\hbar)}{(2-\hbar)W(\hbar)}P_2(t,C) + \frac{2\hbar}{(2-\hbar)W(\hbar)}\int_0^t (P_2(y,\mathcal{V}))dy, \\ \mathcal{I}(t) = \mathcal{I}(0) + \frac{2(1-\hbar)}{(2-\hbar)W(\hbar)}P_3(t,\mathcal{I}) + \frac{2\hbar}{(2-\hbar)(\hbar)}\int_0^t (P_3(y,\mathcal{I}))dy, \\ \mathcal{T}(t) = \mathcal{T}(0) + \frac{2(1-\hbar)}{(2-\hbar)W(\hbar)}P_4(t,\mathcal{R}) + \frac{2\hbar}{(2-\hbar)W(\hbar)}\int_0^t (P_4(y,\mathcal{T}))dy, \\ \mathcal{R}(t) = \mathcal{R}(0) + \frac{2(1-\hbar)}{(2-\hbar)W(\hbar)}P_5(t,\mathcal{V}) + \frac{2\hbar}{(2-\hbar)W(\hbar)}\int_0^t (P_5(y,\mathcal{R}))dy. \end{cases} \tag{4.8}$$

Thus, the above equations yield

$$\left\{\begin{array}{rcl} \mathcal{S}_n(t) &=& 2\frac{(1-\hbar)}{(2-\hbar)W(\hbar)}P_1(t,\mathcal{S}_{(n-1)}) + 2\frac{\hbar}{(2-\hbar)W(\hbar)}\int_0^t (P_1(y,\mathcal{S}_{(n-1)}))dy, \\ \mathcal{V}_n(t) &=& 2\frac{(1-\hbar)}{(2-\hbar)W(\hbar)}P_2(t,\mathcal{V}_{(n-1)}) + 2\frac{\hbar}{(2-\hbar)W(\hbar)}\int_0^t (P_2(y,\mathcal{V}_{(n-1)}))dy, \\ \mathcal{I}_n(t) &=& 2\frac{(1-\hbar)}{(2-\hbar)W(\hbar)}P_3(t,\mathcal{I}_{(n-1)}) + 2\frac{\hbar}{(2-\hbar)W(\hbar)}\int_0^t (P_3(y,\mathcal{I}_{(n-1)}))dy, \\ \mathcal{T}_n(t) &=& 2\frac{(1-\hbar)}{(2-\hbar)W(\hbar)}P_4(t,\mathcal{T}_{(n-1)}) + 2\frac{\hbar}{(2-\hbar)W(\hbar)}\int_0^t (P_4(y,\mathcal{T}_{(n-1)}))dy, \\ \mathcal{R}_n(t) &=& 2\frac{(1-\hbar)}{(2-\hbar)W(\hbar)}P_5(t,\mathcal{R}_{(n-1)}) + 2\frac{\hbar}{(2-\hbar)W(\hbar)}\int_0^t (P_5(y,\mathcal{R}_{(n-1)}))dy, \end{array}\right. \tag{4.9}$$

It has the following initial conditions:

$$\mathcal{S}^0(t) = \mathcal{S}(0), \mathcal{V}^0(t) = \mathcal{V}(0), \mathcal{I}^0(t) = \mathcal{I}(0), \mathcal{T}^0(t) = \mathcal{T}(0), \mathcal{R}^0(t) = \mathcal{R}(0).$$

The difference terms are given by

$$\begin{aligned} \ell_{1n}(t) &= \mathcal{S}_n(t) - \mathcal{S}_{(n-1)}(t) = \frac{2(1-\hbar)}{(2-\hbar)W(\hbar)}(P_1(t,\mathcal{S}_{(n-1)}) - P_1(t,\mathcal{S}_{(n-2)})) \\ &\quad +2\frac{\hbar}{(2-\hbar)W(\hbar)}\int_0^t (P_1(y,\mathcal{S}_{(n-1)}) - P_1(y,\mathcal{S}_{(n-2)}))dy, \\ \ell_{2n}(t) &= \mathcal{V}_n(t) - \mathcal{V}_{(n-1)}(t) = \frac{2(1-\hbar)}{(2-\hbar)W(\hbar)}(P_1(t,\mathcal{V}_{(n-1)}) - P_1(t,\mathcal{V}_{(n-2)})) \\ &\quad +2\frac{\hbar}{(2-\hbar)W(\hbar)}\int_0^t (P_1(y,\mathcal{V}_{(n-1)}) - P_1(y,\mathcal{V}_{(n-2)}))dy, \\ \ell_{3n}(t) &= \mathcal{I}_n(t) - \mathcal{I}_{(n-1)}(t) = \frac{2(1-\hbar)}{(2-\hbar)W(\hbar)}(P_1(t,\mathcal{I}_{(n-1)}) - P_1(t,\mathcal{I}_{(n-2)})) \\ &\quad +2\frac{\hbar}{(2-\hbar)W(\hbar)}\int_0^t (P_1(y,\mathcal{I}_{(n-1)}) - P_1(y,\mathcal{I}_{(n-2)}))dy, \\ \ell_{4n}(t) &= \mathcal{T}_n(t) - \mathcal{T}_{(n-1)}(t) = \frac{2(1-\hbar)}{(2-\hbar)W(\hbar)}(P_1(t,\mathcal{T}_{(n-1)}) - P_1(t,\mathcal{T}_{(n-2)})) \\ &\quad +2\frac{\hbar}{(2-\hbar)W(\hbar)}\int_0^t (P_1(y,\mathcal{T}_{(n-1)}) - P_1(y,\mathcal{T}_{(n-2)}))dy, \\ \ell_{5n}(t) &= \mathcal{R}_n(t) - \mathcal{R}_{(n-1)}(t) = \frac{2(1-\hbar)}{(2-\hbar)W(\hbar)}(P_1(t,\mathcal{R}_{(n-1)}) - P_1(t,\mathcal{R}_{(n-2)})) \\ &\quad +2\frac{\hbar}{(2-\hbar)W(\hbar)}\int_0^t (P_1(y,\mathcal{R}_{(n-1)}) - P_1(y,\mathcal{R}_{(n-2)}))dy. \end{aligned} \tag{4.10}$$

Also, we have the following:

$$\left\{\begin{array}{l} \mathcal{S}_n(t) = \sum_{j=1}^n \ell_{1j}(t), \\ \mathcal{V}_n(t) = \sum_{j=1}^n \ell_{2j}(t), \\ \mathcal{I}_n(t) = \sum_{j=1}^n \ell_{3j}(t), \\ \mathcal{T}_n(t) = \sum_{j=1}^n \ell_{4j}(t), \\ \mathcal{R}_n(t) = \sum_{j=1}^n \ell_{5j}(t). \end{array}\right. \tag{4.11}$$

Similarly, we get that

$$\begin{aligned}\|\ell_{1n}(t)\| &= \|\mathcal{S}_n(t)-\mathcal{S}_{(n-1)}(t)\| = \Big\|2\frac{(1-\hbar)}{(2-\hbar)W(\hbar)}(P_1(t,\mathcal{S}_{(n-1)})-P_1(t,\mathcal{S}_{(n-2)}))\\ &\quad +2\frac{\hbar}{(2-\hbar)W(\hbar)}\int_0^t(P_1(y,\mathcal{S}_{(n-1)})-P_1(y,\mathcal{S}_{(n-2)}))dy\Big\|, \end{aligned} \tag{4.12}$$

$$\begin{aligned}\|\mathcal{S}_n(t)-\mathcal{S}_{(n-1)}(t)\| &\leq 2\frac{(1-\hbar)}{(2-\hbar)W(\hbar)}\|(P_1(t,\mathcal{S}_{(n-1)})-P_1(t,\mathcal{S}_{(n-2)}))\|\\ &\quad +2\frac{\hbar}{(2-\hbar)W(\hbar)}\Big\|\int_0^t(P_1(y,\mathcal{S}_{(n-1)})-P_1(y,\mathcal{S}_{(n-2)}))dy\Big\|. \end{aligned} \tag{4.13}$$

In addition, solving the above Eq (4.13) leads to

$$\begin{aligned}\|\mathcal{S}_n(t)-\mathcal{S}_{n-1}(t)\| &\leq 2\frac{(1-\hbar)}{(2-\hbar)W(\hbar)}Q_1\|\mathcal{S}_{(n-1)}-\mathcal{S}_{(n-2)}\|+2\frac{\hbar}{(2-\hbar)W(\hbar)}Q_1\\ &\quad\times\int_0^t\|\mathcal{S}_{(n-1)}-\mathcal{S}_{(n-2)}\|dy. \end{aligned} \tag{4.14}$$

Therefore,

$$\|\ell_{1n}(t)\| \leq 2\frac{(1-\hbar)}{(2-\hbar)W(\hbar)}Q_1\|\ell_{1(n-1)}(t)\|+2\frac{\hbar}{(2-\hbar)W(\hbar)}Q_1\int_0^t\|\ell_{1(n-1)}(y)\|dy. \tag{4.15}$$

Similarly, we get the results listed below.

$$\begin{aligned}\|\ell_{2n}(t)\| &\leq 2\frac{(1-\hbar)}{(2-\hbar)W(\hbar)}Q_2\|\ell_{2(n-1)}(t)\|+2\frac{\hbar}{(2-\hbar)W(\hbar)}Q_2\int_0^t\|\ell_{2(n-1)}(y)\|dy,\\ \|\ell_{3n}(t)\| &\leq 2\frac{(1-\hbar)}{(2-\hbar)W(\hbar)}Q_3\|\ell_{3(n-1)}(t)\|+2\frac{\hbar}{(2-\hbar)W(\hbar)}Q_3\int_0^t\|\ell_{3(n-1)}(y)\|dy,\\ \|\ell_{4n}(t)\| &\leq \frac{2(1-\hbar)}{(2-\hbar)W(\hbar)}Q_4\|\ell_{4(n-1)}(t)\|+2\frac{\hbar}{(2-\hbar)W(\hbar)}Q_4\int_0^t\|\ell_{4(n-1)}(y)\|dy,\\ \|\ell_{5n}(t)\| &\leq 2\frac{(1-\hbar)}{(2-\hbar)W(\hbar)}Q_5\|\ell_{5(n-1)}(t)\|+2\frac{\hbar}{(2-\hbar)W(\hbar)}Q_5\int_0^t\|\ell_{5(n-1)}(y)\|dy. \end{aligned} \tag{4.16}$$

□

Theorem 4.2. *In the case that the below holds true*

$$2\frac{(1-\hbar)}{(2-\hbar)W(\hbar)}Q_1+2\frac{\hbar}{(2-\hbar)W(\hbar)}Q_1t_0<1,$$

then one can have the exact coupled solutions of the model (9) of COVID-19.

Proof. We observed that the Lipschitz condition is satisfied and the boundedness of $\mathcal{S}(t)$, $\mathcal{V}(t)$, $\mathcal{I}(t),\mathcal{T}(t)$ and $\mathcal{R}(t)$ are ensured. Thus, from Eqs (4.15) and (4.16), we get that

$$\|\ell_{1n}(t)\| \leq \|\mathcal{S}_n(0)\|\Big[\Big(2\frac{(1-\hbar)}{(2-\hbar)W(\hbar)}Q_1\Big)+\Big(2\frac{\hbar}{(2-\hbar)W(\hbar)}Q_1t\Big)\Big]^n,$$

$$
\begin{aligned}
\|\ell_{2n}(t)\| &\leq \|\mathcal{V}_n(0)\|\Big[\Big(2\frac{(1-\hbar)}{(2-\hbar)W(\hbar)}Q_2\Big)+\Big(2\frac{\hbar}{(2-\hbar)W(\hbar)}Q_2t\Big)\Big]^n,\\
\|\ell_{3n}(t)\| &\leq \|\mathcal{I}_n(0)\|\Big[\Big(2\frac{(1-\hbar)}{(2-\hbar)W(\hbar)}Q_3\Big)+\Big(2\frac{\hbar}{(2-\hbar)W(\hbar)}Q_3t\Big)\Big]^n,\\
\|\ell_{4n}(t)\| &\leq \|\mathcal{T}_n(0)\|\Big[\Big(2\frac{(1-\hbar)}{(2-\hbar)W(\hbar)}Q_4\Big)+\Big(2\frac{\hbar}{(2-\hbar)W(\hbar)}Q_4t\Big)\Big]^n,\\
\|\ell_{5n}(t)\| &\leq \|\mathcal{R}_n(0)\|\Big[\Big(2\frac{(1-\hbar)}{(2-\hbar)W(\hbar)}Q_5\Big)+\Big(2\frac{\hbar}{(2-\hbar)W(\hbar)}Q_5t\Big)\Big]^n. \qquad (4.17)
\end{aligned}
$$

From Eq (4.17), we get the existence and continuity of the solution. Now we have to prove Eq (4.17) is a solution of system (9); we start the preceding as follows:

$$
\begin{aligned}
\mathcal{S}(t)-\mathcal{S}(0) &= \mathcal{S}_n(t)-N1_n(t),\\
\mathcal{V}(t)-\mathcal{V}(0) &= \mathcal{V}_n(t)-N2_n(t),\\
\mathcal{I}(t)-\mathcal{I}(0) &= \mathcal{I}_n(t)-N3_n(t),\\
\mathcal{T}(t)-\mathcal{T}(0) &= \mathcal{T}_n(t)-N4_n(t),\\
\mathcal{R}(t)-\mathcal{R}(0) &= \mathcal{R}_n(t)-N5_n(t). \qquad (4.18)
\end{aligned}
$$

Now, we take

$$
\begin{aligned}
\|N1_n(t)\| &= \Big\|\frac{2(1-\hbar)}{(2-\hbar)W(\hbar)}(P_1(t,\mathcal{S}_n)-P_1(t,\mathcal{S}_{(n-1)}))+\frac{2\hbar}{(2-\hbar)W(\hbar)}\times\\
&\quad \int_0^t (P_1(y,\mathcal{S}_n)-P_1(y,\mathcal{S}_{(n-1)}))dy\Big\|,\\
&\leq \frac{2(1-\hbar)}{(2-\hbar)W(\hbar)}\|(P_1(t,\mathcal{S}_n)-(P_1(t,\mathcal{S}_{(n-1)}))\|+\frac{2\hbar}{(2-\hbar)W(\hbar)}\times\\
&\quad \int_0^t \|(P_1(y,\mathcal{S})-P_1(y,\mathcal{S}_{(n-1)}))\|dy,\\
&\leq \frac{2(1-\hbar)}{(2-\hbar)W(\hbar)}Q_1\|\mathcal{S}-\mathcal{S}_{(n-1)}\|+\frac{2\hbar}{(2-\hbar)W(\hbar)}Q_1\|\mathcal{S}-\mathcal{S}_{(n-1)}\|t. \qquad (4.19)
\end{aligned}
$$

Therefore,

$$
\|N1_n(t)\| \leq \Big(\frac{2(1-\hbar)}{(2-\hbar)W(\hbar)}+\frac{2\hbar}{(2-\hbar)W(\hbar)}t\Big)^{n+1}Q_1^{n+1}a. \qquad (4.20)
$$

We attain the following result at time t_0:

$$
\|N1_n(t)\| \leq \Big(\frac{2(1-\hbar)}{(2-\hbar)W(\hbar)}+\frac{2\hbar}{(2-\hbar)W(\hbar)}t_0\Big)^{n+1}Q_1^{n+1}a. \qquad (4.21)
$$

Proceeding in a similar way and using (4.21), we obtain

$$\|N1_n(t)\| \longrightarrow 0, \quad n \to \infty.$$

Similarly, we get that $N2_n(t), N3_n(t), N4_n(t)$ *and* $N5_n(t)$ approaches 0 as n approaches ∞. □

To show that the solution of system (9) is unique, let $(\mathcal{S}_1(t), \mathcal{V}_1(t), \mathcal{I}_1(t), \mathcal{T}_1(t), \mathcal{R}_1(t))$ be any other solution of system (9); then,

$$\begin{aligned} \mathcal{S}(t) - \mathcal{S}_1(t) &= \frac{2(1-\hbar)}{(2-\hbar)W(\hbar)}(P_1(t,\mathcal{S}) - P_1(t,\mathcal{S}_1)) + \frac{2\hbar}{(2-\hbar)W(\hbar)} \\ &\quad \times \int_0^t (P_1(y,\mathcal{S}) - P_1(y,\mathcal{S}_1))\, dy. \end{aligned} \tag{4.22}$$

Taking the norm on both sides of Eq (4.22), we get

$$\begin{aligned} \|\mathcal{S}(t) - \mathcal{S}_1(t)\| &\leq \frac{2(1-\hbar)}{(2-\hbar)W(\hbar)}\|P_1(t,\mathcal{S}) - P_1(t,\mathcal{S}_1)\| + \frac{2\hbar}{(2-\hbar)W(\hbar)} \\ &\quad \times \int_0^t \|P_1(y,S_h) - P_1(y,S_{1h})\| dy. \end{aligned} \tag{4.23}$$

Using the Lipschitz condition, we attain

$$\|\mathcal{S}(t) - \mathcal{S}_1(t)\| \leq \frac{2(1-\hbar)}{(2-\hbar)W(\hbar)} Q_1 \|\mathcal{S}_h(t) - \mathcal{S}_1(t)\| + \frac{2\hbar}{(2-\hbar)W(\hbar)} \times \int_0^t Q_1 t \|\mathcal{S}(t) - \mathcal{S}_1(t)\| dy. \tag{4.24}$$

Hence, we get that

$$\|\mathcal{S}(t) - \mathcal{S}_1(t)\|\Big(1 - \frac{2(1-\hbar)}{(2-\hbar)W(\hbar)} Q_1 - \frac{2\hbar}{(2-\hbar)W(\hbar)} Q_1 t\Big) \leq 0. \tag{4.25}$$

Theorem 4.3. *If the following condition is satisfied:*

$$\Big(1 - \frac{2(1-\ell)}{(2-\ell)U(\ell)} Q_1 - \frac{2\ell}{(2-\ell)\mathcal{U}(\ell)} Q_1 t\Big) > 0, \tag{4.26}$$

then the system (9) has a unique solution.

Proof. Let us suppose that Eq (4.26) holds; then, Eq (4.25) yields the following result:

$$\|\mathcal{S}(t) - \mathcal{S}_1(t)\| = 0, \tag{4.27}$$

Which implies that

$$\mathcal{S}(t) = \mathcal{S}_1(t). \tag{4.28}$$

Similarly we obtain the below listed results

$$\begin{aligned} \mathcal{V}(t) &= \mathcal{V}_1(t), \\ \mathcal{I}(t) &= \mathcal{I}_1(t), \\ \mathcal{T}(t) &= \mathcal{T}_1(t), \\ \mathcal{R}(t) &= \mathcal{R}_1(t). \end{aligned}$$

□

To grasp the dynamical behavior of our COVID-19 model, we chose to run multiple simulations for the suggested fractional system by changing the input parameter values. For simulation proposals, the parameter values listed in Table 1 were utilized, with certain values being assumed in these simulations $\mathcal{S} = 800, \mathcal{V} = 50, \mathcal{I} = 30, \mathcal{T} = 100$ and $\mathcal{R} = 20$, which are the values of state variables.

We ran four distinct scenarios to see how different settings affect the system's output. Our major goal was to detect the level of infection and the volatility of these values, as well as to anticipate appealing control measures for COVID-19 infection prevention. In the first instance, we show how fractional order affects the system shown in Figures 4–5. In these simulations, we primarily focused on the system's variation in response to changes in the index of memory. We observed that this input factor has a significant influence on the system and can effectively decrease the level of infection in the community. In Figure 6, we varied the value of the transmission rate ω; thus, we can observe the fluctuation of the dynamics in the second scenario. In the third and fourth scenarios respectively presented in Figures 7 and 8, we show the dynamical behavior of the hypothesized model with the variation in treatment and vaccination rates ρ and γ, respectively; we noticed the influence of each of these parameters on the infected individuals in the COVID-19 model. In our results, we observed that the vaccination rate has an attractive influence on the system in terms of its ability to reduce the level of infection; thus, it can be used as a control parameter. Finally, regarding in the last scenario, the efficacy loss rate of vaccination is illustrated in Figure 9 which shows that this factor is critical and can increase the risk of infection.

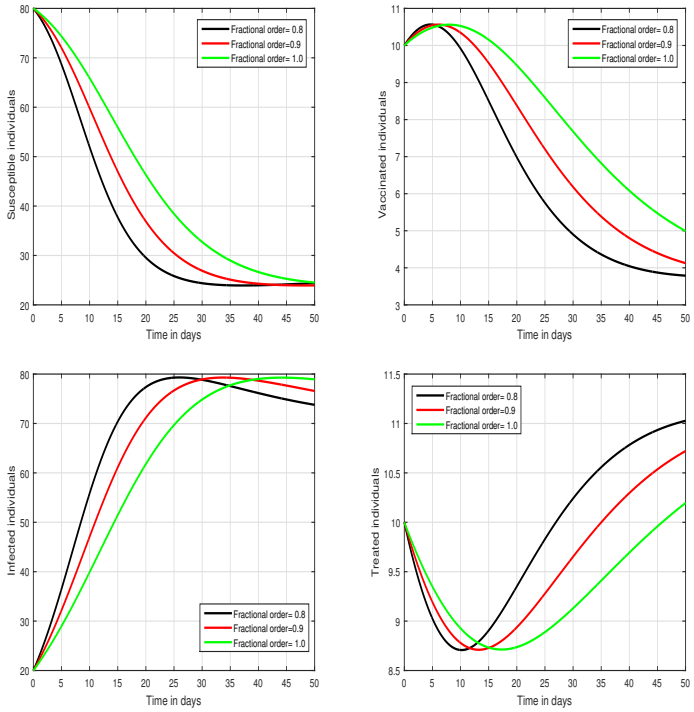

Figure 4. Tracking path analysis of (6) of COVID-19 infection with various values of $\hbar$, i.e., $\hbar = 1.0, 0.9, 0.8$.

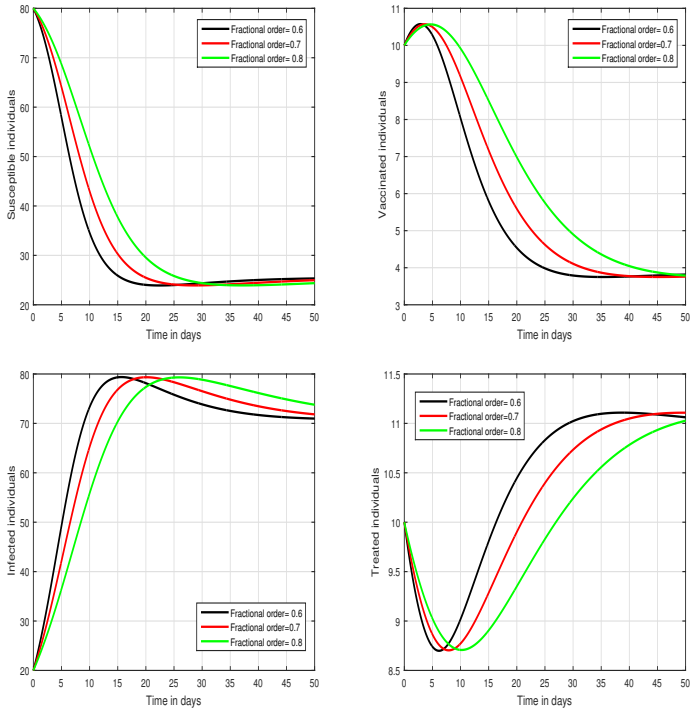

Figure 5. Tracking path behavior of (6) of COVID-19 infection with various values of $\hbar$, i.e., $\hbar = 0.8, 0.7, 0.6$.

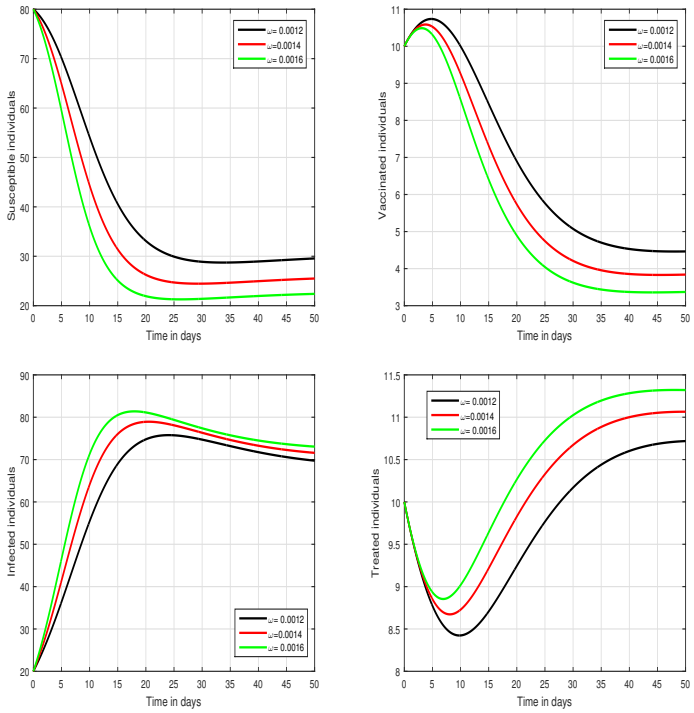

Figure 6. Representation of the time series of our model (6) of COVID-19 infection with the variation of ω, i.e., $\omega = 0.0012, 0.0014, 0.0016$.

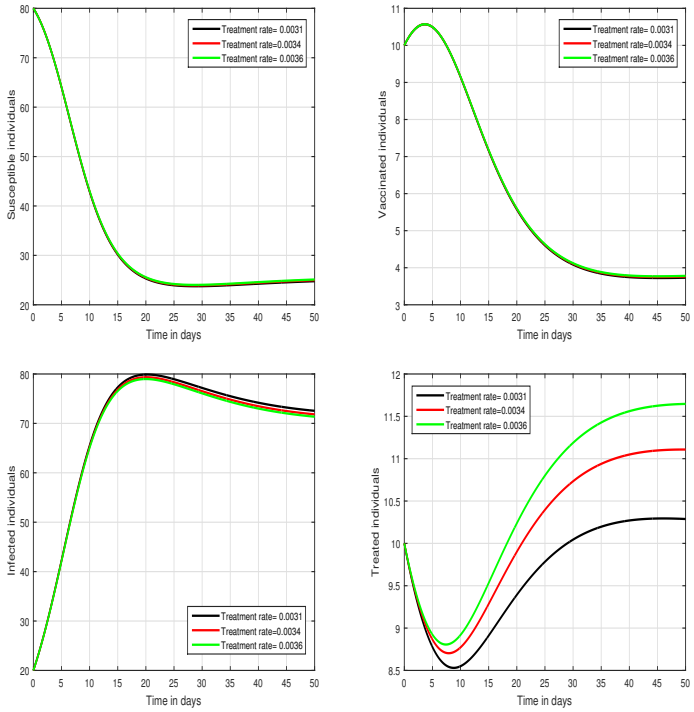

Figure 7. Representation of the time series of our model (6) of COVID-19 infection with various values of the input parameter ρ, i.e., $\rho = 0.0031, 0.0034, 0.0036$.

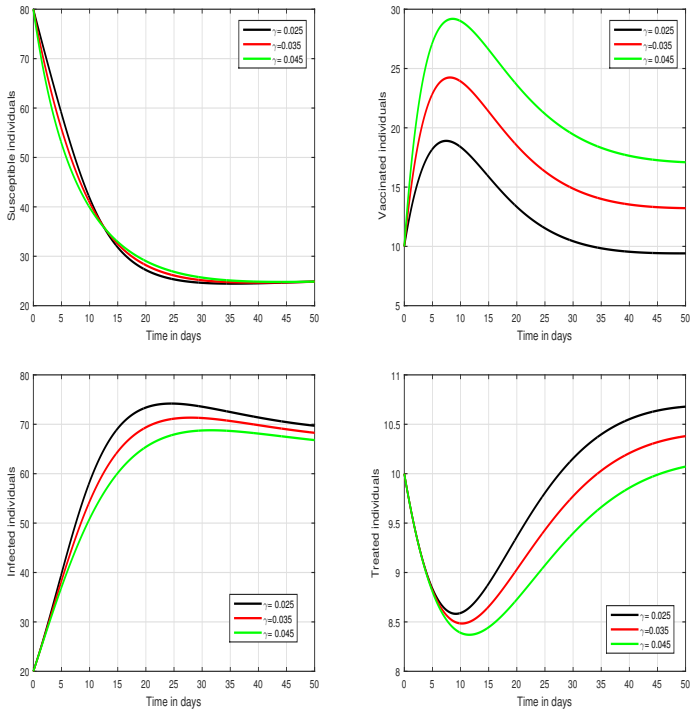

Figure 8. Graphical representation of the time series of (6) of COVID-19 infection with the various values of the input parameter γ, i.e., $\gamma = 0.025, 0.035, 0.045$.

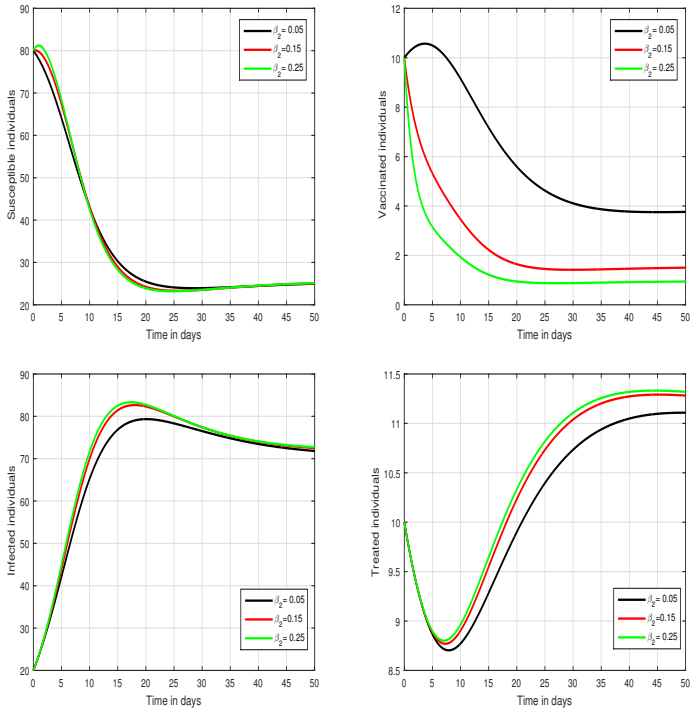

Figure 9. Graphical representation of the time series of (6) of COVID-19 infection with different values of vaccine loss efficacy β_2, i.e., $\beta_2 = 0.05, 0.15, 0.25$.

5. Conclusions

In the context of the CF derivative, we introduced a mathematical model for the COVID-19 transmission process incorporating vaccination and therapy components. For the examination of the recommended dynamics, we represented the fundamental findings of fractional theory. We examined the steady states of the system and the reproduction parameter $\mathcal{R}_0$ was calculated via a next-generation matrix approach. The infection-free equilibrium of the suggested system has been determined to be locally asymptotically stable if $\mathcal{R}_0 < 1$ and unstable in all other cases. It has been proved that the endemic steady state is locally asymptotically stable for $\mathcal{R}_0 > 1$. The system's reproduction parameter has been quantitatively explored by varying various factors. In addition to this, we established results for the existence and uniqueness of the solution for the proposed COVID-19 infection model. The tracking path behavior of our model has been analyzed by using a numerical method. Numerical simulations with different input parameters have been used to show the system's dynamical behavior. The influence of various factors of the system has been conceptualized for the solution pathways. For infection control, the most significant scenario of the system has been proposed to the public health. In the future work, the dynamics of COVID-19 infection will be examined through the use of stochastic differential equations. Moreover, we will also apply real data to the dynamics of COVID-19 infection for further predictions.

Acknowledgments

The authors extend their appreciation to the Deanship of Scientific Research at King Khalid University for funding this work through the Research Groups Program [grant number R.G.P.2/25/44].

Conflict of interest

The authors stated that there are no conflicts of interest regarding this work.

References

1. V. D. Ashwlayan, C. Antlash, M. Imran, S. M. B. Asdaq, M. K. Alshammari, M. Alomani, et al., Insight into the biological impact of COVID-19 and its vaccines on human health, *Saudi J. Biol. Sci.*, **29** (2022), 3326–3337. https://doi.org/10.1016/j.sjbs.2022.02.010
2. A. I. Shahin, S. Almotairi, A deep learning BiLSTM encoding-decoding model for COVID-19 pandemic spread forecasting, *Fractal Fract.*, **5** (2021), 175. https://doi.org/10.3390/fractalfract5040175
3. J. Wang, J. Pang, X. Liu, Modelling diseases with relapse and nonlinear incidence of infection: a multi-group epidemic model, *J. Biol. Dynam.*, **8** (2014), 99–116. https://doi.org/10.1080/17513758.2014.912682
4. N. Ma, W. Ma, Z. Li, Multi-model selection and analysis for COVID-19, *Fractal Fract.*, **5** (2021), 120. https://doi.org/10.3390/fractalfract5030120
5. R. Jan, S. Boulaaras, Analysis of fractional-order dynamics of dengue infection with non-linear incidence functions, *T. I. Meas. Control*, **44** (2022). https://doi.org/10.1177/01423312221085049
6. S. Boulaaras, R. Jan, A. Khan, M. Ahsan, Dynamical analysis of the transmission of dengue fever via Caputo-Fabrizio fractional derivative, *Chaos Soliton. Fract.*, **8** (2022), 100072. https://doi.org/10.1016/j.csfx.2022.100072
7. K. Prem, Y. Liu, T. W. Russell, A. J. Kucharski, R. M. Eggo, N. Davies, et al., The effect of control strategies to reduce social mixing on outcomes of the COVID-19 epidemic in Wuhan, China: a modelling study, *Lancet Public Health*, **5** (2020), e261–e270. https://doi.org/10.1016/S2468-2667(20)30073-6
8. N. Lurie, M. Saville, R. Hatchett, J. Halton, Developing COVID-19 vaccines at pandemic speed, *New Eng. J. Med.*, **382** (2020), 1969–1973. https://doi.org/10.1056/NEJMp2005630
9. F. Amanat, F. Krammer, SARS-CoV-2 vaccines: status report, *Immunity*, **52** (2020), 583–589. https://doi.org/10.1016/j.immuni.2020.03.007
10. J. E. Aledort, N. Lurie, J. Wasserman, S. A. Bozzette, Non-pharmaceutical public health interventions for pandemic influenza: an evaluation of the evidence base, *BMC Public Health*, **7** (2007), 1–9. https://doi.org/10.1186/1471-2458-7-208
11. T. M. Chen, J. Rui, Q. P. Wang, Z. Y. Zhao, J. A. Cui, A mathematical model for simulating the phase-based transmissibility of a novel coronavirus, *Infect. Dis. Poverty*, **9** (2020), 24. https://doi.org/10.1186/s40249-020-00640-3

12. M. A. Khan, A. Atangana, Modeling the dynamics of novel coronavirus (2019-nCov) with fractional derivative, *Alex. Eng. J.*, **59** (2020), 2379–2389. https://doi.org/10.1016/j.aej.2020.02.033
13. J. M. Read, J. R. Bridgen, D. A. Cummings, A. Ho, C. P. Jewell, Novel coronavirus 2019-nCoV: Early estimation of epidemiological parameters and epidemic predictions, *Philos. T. R. Soc. B*, **376** (2020). https://doi.org/10.1098/rstb.2020.0265
14. A. R. Tuite, D. N. Fisman, A. L. Greer, Mathematical modelling of COVID-19 transmission and mitigation strategies in the population of Ontario, *CMAJ*, **192** (2020), E497–E505. https://doi.org/10.1503/cmaj.200476
15. O. Pinto Neto, D. M. Kennedy, J. C. Reis, Y. Wang, A. C. B. Brizzi, G. J. Zambrano, et al., Mathematical model of COVID-19 intervention scenarios for Sao PauloBrazil, *Nat. Commun.*, **12** (2021), 418. https://doi.org/10.1038/s41467-020-20687-y
16. O. Nave, U. Shemesh, I. HarTuv, Applying Laplace Adomian decomposition method (LADM) for solving a model of COVID-19, *Comput. Method. Biomec.*, **24** (2021), 1618–1628. https://doi.org/10.1080/10255842.2021.1904399
17. Z. Shah, R. Jan, P. Kumam, W. Deebani, M. Shutaywi, Fractional dynamics of HIV with source term for the supply of new CD4+ T-cells depending on the viral load via Caputo-Fabrizio derivative, *Molecules*, **26** (2021), 1806. https://doi.org/10.3390/molecules26061806
18. T. Q. Tang, Z. Shah, R. Jan, E. Alzahrani, Modeling the dynamics of tumorimmune cells interactions via fractional calculus, *Eur. Phys. J. Plus*, **137** (2022), 367. https://doi.org/10.1140/epjp/s13360-022-02591-0
19. S. Qureshi, A. Yusuf, Fractional derivatives applied to MSEIR problems: comparative study with real world data, *Eur. Phys. J. Plus*, **134** (2019), 171. https://doi.org/10.1140/epjp/i2019-12661-7
20. S. Qureshi, R. Jan, Modeling of measles epidemic with optimized fractional order under Caputo differential operator, *Chaos Soliton. Fract.*, **145** (2021), 110766. https://doi.org/10.1016/j.chaos.2021.110766
21. S. Kumar, R. P. Chauhan, S. Momani, S. Hadid, Numerical investigations on COVID-19 model through singular and non-singular fractional operators, *Numer. Meth. Part. Differ. Equ.*, 2020. https://doi.org/10.1002/num.22707
22. A. Atangana, S. İĞret araz, A novel COVID-19 model with fractional differential operators with singular and non-singular kernels: analysis and numerical scheme based on Newton polynomial, *Alex. Eng. J.*, **60** (2021), 3781–3806. https://doi.org/10.1016/j.aej.2021.02.016
23. R. Jan, A. Khurshaid, H. Alotaibi, M. Inc, A robust study of the transmission dynamics of syphilis infection through non-integer derivative, *AIMS Math.*, **8** (2023), 6206–6232. https://doi.org/10.3934/math.2023314
24. O. A. Omar, R. A. Elbarkouky, H. M. Ahmed, Fractional stochastic modelling of COVID-19 under wide spread of vaccinations: Egyptian case study, *Alex. Eng. J.*, **61** (2022), 8595–8609. https://doi.org/10.1016/j.aej.2022.02.002
25. O. A. Omar, Y. Alnafisah, R. A. Elbarkouky, H. M. Ahmed, COVID-19 deterministic and stochastic modelling with optimized daily vaccinations in Saudi Arabia, *Results Phys.*, **28** (2021), 104629. https://doi.org/10.1016/j.rinp.2021.104629

26. M. Caputo, M. Fabrizio, A new definition of fractional derivative without singular kernel, *Progr. Fract. Differ. Appl.*, **1** (2015), 73–85. http://dx.doi.org/10.12785/pfda/010201
27. J. Losada, J. J. Nieto, Properties of a new fractional derivative without singular kernel, *Progr. Fract. Differ. Appl.*, **1** (2015), 87–92. http://dx.doi.org/10.12785/pfda/010202
28. R. Jan, M. A. Khan, Y. Khan, S. Ullah, A new model of dengue fever in terms of fractional derivative, *Math. Biosci. Eng.*, **17** (2020), 5267–5288.
29. P. Van den Driessche, J. Watmough, Reproduction numbers and sub-threshold endemic equilibria for compartmental models of disease transmission, *Math. Biosci.*, **180** (2002), 29–48. https://doi.org/10.1016/S0025-5564(02)00108-6
30. C. Castillo-Chavez, Z. Feng, W. Huang, On the computation of R0 and its role on global stability, Mathematical approaches for emerging and re-emerging infection diseases: an introduction, **125** (2002), 31–65.

AIMS Press